

Surface Fractal Properties of Morphologically Different Sol–Gel Derived Silicates

Á. Kukovecz,^{*,†} Z. Kónya,[†] I. Pálincó,[‡] D. Mönter,[§] W. Reschetilowski,[§] and I. Kiricsi[†]

Department of Applied and Environmental Chemistry, University of Szeged, Rerrich Béla tér 1, H-6720 Szeged, Hungary, Department of Organic Chemistry, University of Szeged, H-6720 Szeged, Dóm tér 8, Hungary, and Institut für Technische Chemie, Technische Universität Dresden, Mommsenstrasse 4, 01062 Dresden, Germany

Received August 24, 2000. Revised Manuscript Received October 23, 2000

Silica nanotubes, foams and ordinary mesoporous silica have been synthesized by the controlled hydrolysis of tetraethyl orthosilicate in the presence of various organic agents. The effects of mechanical pressure were studied by subjecting the samples up to 9 ton/cm² pressure. Surface fractal properties were investigated by analysis of the N₂ adsorption–desorption isotherms by the Frenkel–Halsey–Hill equation and the Wang method. We have found that while amorphous mesoporous silica has a definitely self-similar surface, silica nanotubes and foams can be considered nonfractal with $D_{\text{fract}} \sim 2$ and $D_{\text{fract}} \sim 3$, respectively.

Introduction

The rapid development of the sol–gel technique¹ in recent years has directed a large research effort toward the synthesis of solids possessing nonconventional pore structures. New zeolite types,² nanotubes,³ foams,⁴ and coatings⁵ could all be prepared by the controlled hydrolysis of silicon alkoxides. Apart from being interesting in their own right, such materials may well find applications in heterogeneous catalysis,⁶ shape-selective molecular sieving,⁷ or biocomposites.⁸ A field that could benefit especially from the control over activity and morphology⁹ offered by the sol–gel technique is solid membrane science, which could use tailor-made silica foam monoliths instead of laboriously grown zeolite films,¹⁰ for example.

Fractal analysis has become a very popular tool in solid surface characterization in the last two decades.^{11–14} Fractal materials have scale-invariant morphological

features by definition and can be classified¹⁵ as mass fractals, pore fractals, and surface fractals. From the point of view of heterogeneous catalysis, the latter two are of considerable interest, since transport efficiency¹⁶ and catalytic activity^{14,17} may both be related to pore and surface self-similarity. Because of their paramount importance in separation, adsorption, and catalysis, the fractality of silica species has been quite extensively studied^{18–22} already. While it is generally agreed¹⁶ that pore fractals are rarely found among common porous materials, the existence of surface fractality in silica specimens is still heavily debated. Even by narrowing the scope of investigation down to sol–gel-derived silicas we can find a wide range of opinions ranging from the denial (“...it is more realistic to assume that a given porous system does not show a fractal structure”; Gottsleben and Hesse²³) to the acceptance (numerous authors have calculated fractal dimensions for such species; e.g., Sermon et al.²¹) of the surface fractality of these materials.

In this paper we present a comprehensive study on the surface scale invariance of certain sol–gel-derived silica species, propose a new mechanism for silica nanotube formation, and prove that surface fractality depends at least as heavily on morphological issues as on elemental composition. Additionally, we shall investigate the effects of mechanical pressure on surface

* Corresponding author: Tel/fax +36 62 544 619; e-mail kakos@chem.u-szeged.hu.

[†] Department of Applied and Environmental Chemistry, University of Szeged.

[‡] Department of Organic Chemistry, University of Szeged.

[§] Technische Universität Dresden.

- (1) Hench, L. L.; West, J. K. *Chem. Rev.* **1990**, *90*, 33.
- (2) Barrett, P. A.; Camblor, M. A.; Corma, A.; Jones, R. H.; Villaescusa, L. A. *Chem. Mater.* **1997**, *9*, 1713.
- (3) Nakamura, H.; Matsui, Y. *J. Am. Chem. Soc.* **1995**, *117*, 2651.
- (4) Bagshaw, S. A. *Chem. Commun.* **1999**, 767.
- (5) Yamazaki, S.; Tsutsumi, K. *Microporous Mater.* **1995**, *4*, 205.
- (6) Lange, C.; Storck, S.; Tesche, B.; Maier, W. F. *J. Catal.* **1998**, *175*, 280.
- (7) Sano, T.; Yanagishita, H.; Kiyozumi, Y.; Mizukami, F.; Haraya, K. *J. Membr. Sci.* **1994**, *95*, 221.
- (8) Jain, T. K.; Roy, I.; De, T. K.; Maitra, A. *J. Am. Chem. Soc.* **1998**, *120*, 11092.
- (9) Ward, D. A.; Ko, E. I. *Ind. Eng. Chem. Res.* **1995**, *34*, 421.
- (10) Boudreau, L. C.; Tsapatsis, M. *Chem. Mater.* **1997**, *9*, 1705.
- (11) Pfeifer, P.; Avnir, D.; Farin, D. *J. Chem. Phys.* **1983**, *79*, 3666.
- (12) Pfeifer, P.; Avnir, D. *Nature* **1984**, *208*, 261.
- (13) Ehrburger-Dolle, F.; Holz, M.; Lahaye, J. *Pure Appl. Chem.* **1993**, *65*, 2223.
- (14) Rigby, S. P.; Gladden, L. F. *J. Catal.* **1998**, *180*, 44.

(15) Avnir, D., Ed. *The Fractal Approach to Heterogeneous Chemistry*; Wiley: New York, 1992.

(16) Conner, W. C.; Bennett, C. O. *J. Chem. Soc., Faraday Trans.* **1993**, *89*, 4109.

(17) Giona, M.; Giustiniani, M. *J. Phys. Chem.* **1996**, *100*, 16690.

(18) Ehrburger-Dolle, F. *Langmuir* **1997**, *13*, 1189.

(19) Fadeev, A. Y.; Borisova, O. R.; Lisichkin, G. V. *J. Colloid Interface Sci.* **1996**, *183*, 1.

(20) Wang, F.; Li, S. *Ind. Eng. Chem. Res.* **1997**, *36*, 1598.

(21) Sermon, P. A.; Wang, Y.; Vong, M. S. W. *J. Colloid Interface Sci.* **1994**, *168*, 327.

(22) Drake, J. M.; Levitz, P.; Klafter, J. *New J. Chem.* **1990**, *14*, 77.

(23) Gottsleben, F.; Hesse, D. *Hung. J. Ind. Chem.* **1991**, *19*, 283.

fractality, which is considered to be important from the practical point of view, e.g., in the preparation of disk-shaped catalysts used in fixed bed flow reactors.

Experimental Section

Preparation of the Porous Solids. For the synthesis of ordinary amorphous mesoporous silicates, 13.86 g of tetraethyl orthosilicate (TEOS) was dissolved in 8 g of ethanol and 8.26 g of ethylene glycol with stirring at 353 K in an oil bath. After 1 h of stirring, a mixture of 24 g of ethanol, 6 g of water, and a catalytic amount of acetic acid was added to the system. The stirring rate and temperature were maintained long enough (typically 3 h) to reach a clear, transparent, solid gel state. The resulting gel was aged at ambient conditions for 24 h and dried under reduced pressure at 413 K for 3 h.

Silica nanotubes were prepared at ambient conditions by the method described by Nakamura and Matsui.³ We have found that it is possible to scale up the original process while maintaining a constant nanotube yield. The reaction was carried out as follows: 10.0 g of DL-tartaric acid and 30.0 g of water were dissolved in 2000 mL of absolute ethanol. To this solution 365 g of TEOS was added and the mixture was stirred for 5 min with a magnetic stirrer. After that, the system was allowed to stand for 30 min and then 1000 mL of 25% NH₃ solution was added, while being stirred lightly by a glass rod. In about 15 s an opal white gel was formed, which was permitted to stand for 20 min and then was washed with water to remove excess NH₃ and dried at 378 K overnight.

Macrocellular mesoporous silicate foams were prepared by a modified sol-gel route based on the technique suggested by Bagshaw.⁴ Triton X-114 (a nonionic surfactant from Fluka) (4.58 g) was dissolved in 30 g of H₂O adjusted to pH = 1 by addition of a few drops of H₂SO₄. This solution was stirred at ambient conditions at 500 rpm by a magnetic stirrer for 1 h and then 13.86 g of TEOS was added to the foam. Stirring was maintained until a thick white gel was formed (4–6 h). The gel was transferred into a Petri dish and allowed to age overnight. Half of the resulting foam monolith was hydrothermally treated at 413 K for 24 h, while the other half was dried at 313 K for 24 h. Finally, all samples were calcined at 773 K for 12 h in a flow of O₂.

The effects of mechanical pressure were studied for each material by applying 0, 3, and 9 ton/cm² pressure to 200 mg of sample for 2 min.

Characterization of the Samples. N₂ adsorption-desorption isotherms were measured at 77 K in a volumetric apparatus. About 100 mg of sample, outgassed in vacuum at 723 K for 1 h, was used for each experiment. Optical photographs were obtained by a Nikon binocular microscope equipped with a normal 35 mm Nikon camera. SEM images were recorded on a Philips instrument.

Determination of the Fractal Dimension. Ever since the introduction of the fractal concept to heterogeneous chemistry,¹¹ the most widespread methods for the calculation of surface fractal dimension have been based on adsorption measurements. One either measures the variation in the surface area when determined by use of a series of adsorbents (e.g., *n*-alkanes)¹² or determines the surface roughness from the data contained in one adsorption isotherm. In this contribution we present results based on the latter approach. The N₂ adsorption isotherms described above have been analyzed both by the Frenkel-Halsey-Hill (FHH) equation¹³ and by the Wang method.²⁰

The FHH equation can be expressed as

$$\ln N = \text{const} - (3 - D) \ln \mu \quad (1)$$

where *N* is the amount adsorbed at the relative pressure *P/P*₀ (the range 0.35 < *P/P*₀ < 0.75 has been used for the determination of *D*) and absolute temperature *T*, *D* is the surface

fractal dimension and μ is the adsorption potential defined as

$$\mu = RT \ln(P_0/P) \quad (2)$$

The calculation suggested by Wang and Li²⁰ is a development of the so-called thermodynamic method first described by Neimark.²⁴ The *D* surface fractal dimension can be calculated from the data in the region of capillary condensation (the whole *P/P*₀ > 0.35 region can be used for the calculation) of both the adsorption and desorption branches of an isotherm by use of the following relationship:

$$\ln A(X) = \text{const} + D \ln B(X) \quad (3)$$

where *X* denotes the relative pressure *P/P*₀ and *A(X)* and *B(X)* are defined as

$$A(X) = \frac{\int_{N(X)}^{N_{\max}} \ln X \, dN(X)}{r_c^2(X)} \quad (4)$$

In these equations *N*_{max} denotes the amount adsorbed at *X*

$$B(X) = \frac{[N_{\max} - N(X)]^{1/3}}{r_c(X)} \quad (5)$$

tending to unity, and *r*_c(*X*) can be calculated from the Kelvin equation:

$$r_c = \frac{-2\sigma V_L}{RT \ln X} \quad (6)$$

where σ denotes the surface tension between liquid and gas-phase nitrogen, and *V*_L stands for the molar volume of liquid nitrogen.

Errors in the data presented in Tables 1–5 have been calculated at 95% significance level assuming normal error distribution.

Results

SEM images of the xerogels presented in Figure 1 reveal three totally different morphological classes. While samples synthesized in the presence of alcohols only are completely amorphous, those originating from DL-tartaric acid-containing precursors are made of silica nanotubes, and the addition of Triton X-114 directed gelation toward a foam shape indeed. It should be noted that another phase consisting of aggregated nonporous silica spheres has also been formed along with the nanotubes. On the basis of SEM pictures we estimate the average silica nanotube to have an outer diameter of 0.8–1.5 μ m, inner diameter of 0.5–0.8 μ m, and length of 5–100 μ m and the nanotube/aggregate ratio to be above 5. The silica foam was obtained as a monolith (apparent density after calcination \sim 0.08 g/cm³) sharing dimensions with the synthesis vessel. The diameter of the observed foam pores ranged from 4–6 mm to 2–5 μ m. However, we are quite positive about the existence of even narrower pores, which could not be identified clearly because of instrumental limitations. The hydrothermal treatment had no direct effect on foam morphology.

The major characteristics of the pore structure of each sample are presented in Table 1 as calculated from the N₂ adsorption isotherms. As expected, silica foams have the largest and silica nanotubes the smallest BET area.

(24) Neimark, A. *Physica A* **1992**, *191*, 258.

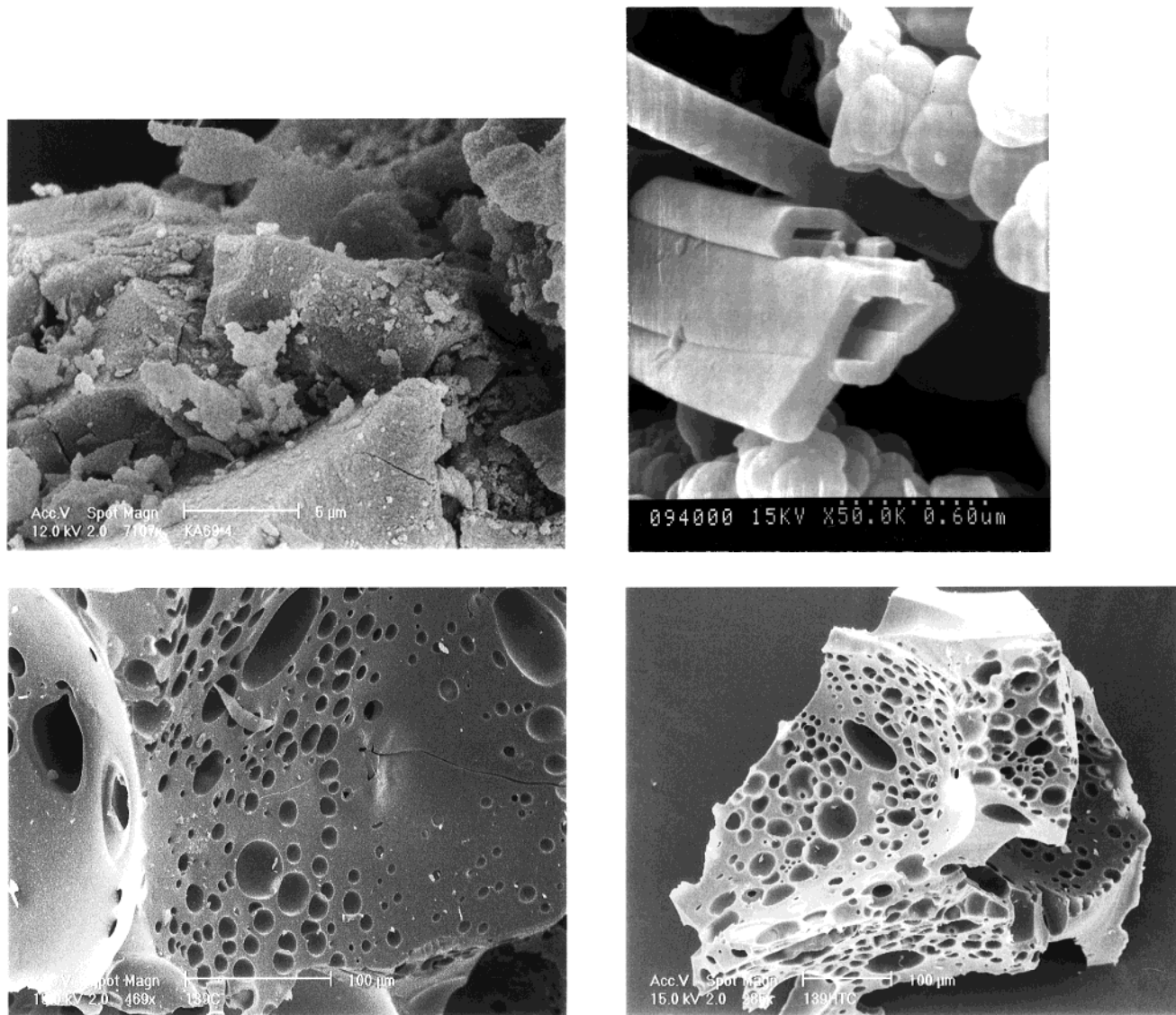


Figure 1. Typical SEM images of the materials discussed. (a, upper left) Amorphous silica; (b, upper right) silica nanotube; (c, lower left) original silica foam; (d, lower right) hydrothermally treated silica foam.

Table 1. Major Characteristics of the Pore Structure of the Materials Studied

	BET surface area (m ² /g)	pore diameter ^a (Å)	pore volume (mL/g)	micropore volume ^b (mL/g)
amorphous silica	297 ± 4	18 ± 2	0.47 ± 0.03	0.1167 ± 0.0074
nanotube	24 ± 2	1720 ± 61	0.26 ± 0.03	0.0018 ± 0.0002
original foam	863 ± 6	36 ± 3	0.78 ± 0.15	0.064 ± 0.005
hydrothermally treated foam	779 ± 6	43 ± 4	0.91 ± 0.22	0.053 ± 0.003

^a Abscissa of the maximum of the pore size distribution curve calculated by the BJH method. ^b Calculated by the Dubinin–Rudusckevich method.

Pore size distribution calculations utilizing the Barret–Joyner–Halenda method indicate that nanotubes can be considered as essentially macroporous materials, while the majority of the pores of amorphous silica and silica foam falls in the mesoporous range. Micropores can also be found, primarily in the amorphous silica bulk.

The surface fractal dimension calculated by both methods and at all three pressures applied is given for amorphous silica, silica nanotube, and original and hydrothermally treated silica foam in Tables 2–5, respectively. It is easy to notice that the general fractal

Table 2. Surface Fractal Dimension of Amorphous Silica

applied pressure (ton/cm ²)	Wang method		FHH equation	
	adsorption	desorption	adsorption	desorption
0	2.38 ± 0.07	2.61 ± 0.10	2.48 ± 0.12	2.53 ± 0.08
3	2.41 ± 0.03	2.67 ± 0.08	2.47 ± 0.04	2.52 ± 0.05
9	2.58 ± 0.05	2.64 ± 0.06	2.34 ± 0.07	2.39 ± 0.11

behavior is independent of the details of the calculation and that D is approximately 2 for nanotubes, 3 for foams, and ca. 2.5 for amorphous silica. The latter material did not exhibit any change in surface fractal dimension up to 9 ton/cm², but in the case of nanotubes

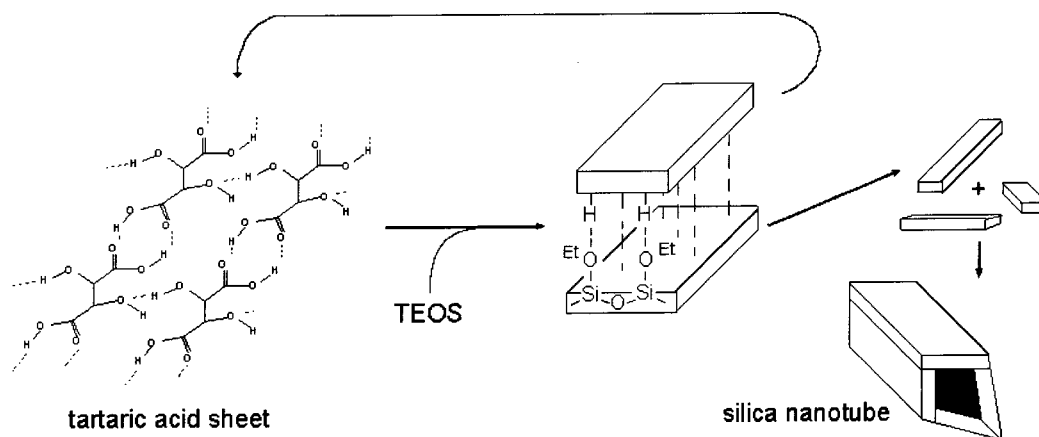


Figure 2. Suggested mechanism of the formation of silica nanotubes having angular cross-sections.

Table 3. Surface Fractal Dimension of Silica Nanotube

applied pressure (ton/cm ²)	Wang method		FHH equation	
	adsorption	desorption	adsorption	desorption
0	2.02 ± 0.11	2.08 ± 0.14	2.15 ± 0.04	2.07 ± 0.02
3	2.06 ± 0.10	2.10 ± 0.07	2.03 ± 0.06	2.11 ± 0.12
9	2.16 ± 0.05	2.23 ± 0.09	2.14 ± 0.05	2.16 ± 0.08

Table 4. Surface Fractal Dimension of Original Silica Foam

applied pressure (ton/cm ²)	Wang method		FHH equation	
	adsorption	desorption	adsorption	desorption
0	2.89 ± 0.11	2.97 ± 0.15	2.92 ± 0.17	2.99 ± 0.10
3	2.86 ± 0.17	2.98 ± 0.18	2.93 ± 0.19	2.86 ± 0.14
9	2.79 ± 0.15	2.81 ± 0.15	2.84 ± 0.12	2.85 ± 0.16

Table 5. Surface Fractal Dimension of Hydrothermally Treated Silica Foam

applied pressure (ton/cm ²)	Wang method		FHH equation	
	adsorption	desorption	adsorption	desorption
0	2.93 ± 0.15	2.91 ± 0.09	2.98 ± 0.12	2.93 ± 0.16
3	2.90 ± 0.08	2.89 ± 0.07	2.88 ± 0.03	2.88 ± 0.11
9	2.85 ± 0.06	2.83 ± 0.13	2.77 ± 0.10	2.82 ± 0.14

and foams a small shift toward $D = 2.5$ could be observed. It should also be noted that the foam structure collapsed completely even at pressures below 1 ton/cm².

Discussion

The amorphous nature of the simple mesoporous silica sample is in good agreement with data reported in the literature. Its typical grain size of 2–20 μm indicates that the primary morphological control factors must have been gel shrinkage and grinding. However, the visible surface of the grains is rather complex, which can be interpreted by assuming that the hydrolysis rate of TEOS and the aggregation of the primary sol nanoparticles play a dominant role in developing the final surface features of the material.

Silica nanotubes, on the other hand, exhibit practically no surface anomalies, only smooth flat walls. Besides the tubular shape, their key morphological feature is that they have an angular cross section instead of a circular one. The origin of this rather unusual (compared, e.g., to the well-known circular carbon nanotubes) property is currently being debated.

It is clear that because of its small size DL-tartaric acid cannot play the role of a conventional template molecule. Nakamura and Matsui³ suggested that a ladder-like structure is formed from D- and L-tartaric acid molecules to serve as supramolecular template. However, it is rather dubious if the small amount of DL-tartaric acid in the precursor solution can validate any model that assumes a fixed template–silica interaction. In our opinion, tartaric acid molecules form quasi-flat sheets that can serve as templates for flat silica panels. After reaching a certain size, the silica planes are detached from the tartaric acid sheet, which becomes ready for directing the formation of the next plane. The nanotube formation is a secondary process occurring spontaneously when two planes meet. The steps of this proposed mechanism are visualized in Figure 2.

Silica foam formation seems to be more straightforward to explain: TEOS hydrolysis takes place in the walls of the foam raised by the heavy stirring of the aqueous detergent solution. A comprehensive discussion of the phenomenon was given by Bagshaw.³ However, silica foams could be very interesting from the fractal point of view. We think that they might fulfill the prerequisites set forth for pore fractals by Conner and Bennett.¹⁶ This would call for detailed investigations, since up till now only very few real pore fractal materials have been found. Unfortunately, such studies are out of the scope of the present paper.

The surface fractal dimension (D) of a solid is basically an indicator of the presence (or absence) of scale invariant surface features. The case of $D = 2$ corresponds to adsorption on a smooth, flat surface. $D = 3$ indicates space filling with the adsorbate, while cases of $2 < D < 3$ conform to adsorption on a fractal surface. The surface fractal dimension of freshly calcined silica nanotubes was found to be close to 2, independent of the method of calculation. No scale-invariant features are present: the word "surface" can only be interpreted on one scale, and that is the micrometer dimensional scale of the tubes. (The surface area—and thus the contribution to the surface fractal dimension measurable by adsorption techniques—of the aggregated silica phase is negligible²⁵ compared to that of the nanotubes.)

(25) Ströber, W.; Fink, A.; Bohn, E. *J. Colloid Interface Sci.* **1968**, *26*, 62.

This finding is consistent with the formation mechanism suggested above: the nanotubes are made of silica planes of roughly the same size, which is easiest to explain by assuming that a large number of planes are synthesized on the very same template sheet. While moderate mechanical pressure has no effect on the fractality of the nanotubes, applying a large pressure of 9 ton/cm² resulted in a minor increase in D . The increase is probably caused by physical fracture effects. The walls of the nanotubes break, and the revealed jagged surfaces have adsorption properties different from the original smooth tube walls. Since the majority of these planes remains intact, the overall observable result is the ~ 0.1 increase in the surface fractal dimension.

The $D \sim 3$ values obtained for the calcined silica foam indicate that this material also lacks fractal surface features, but for a completely different reason. Here the adsorption process quickly changed to space filling, and therefore the formalism of eqs 1 and 3 can no longer provide information about *surface* properties. As mentioned above, we believe that such foams could be pore fractals, and in that respect it is quite understandable that they do not exhibit surface and pore fractality at the same time. Our foam proved to be extremely vulnerable to mechanical pressure, as even at 1 ton/cm² it has lost its hollow structure and was pressed into white powder. This denser material no longer exhibited space-filling adsorption capabilities; instead, it started behaving as a fractal surface of $D \sim 2.8$. In our opinion, this transition originates from the appearance of a new type of surface, which is made up of the tightly compressed shells of the foam pores.

The ordinary amorphous mesoporous silica sample was found to be a surface fractal in the submicrometer dimension by all calculation methods and at all pressures applied. Once again, the synthesis conditions,

namely, the possibility for the secondary aggregation of the sol particles, seem to be responsible for this phenomenon. Effects of the mechanical pressure are hardly identifiable: the material was lacking morphology right after calcination, and therefore even the 9 ton/cm² pressure could only transform it from one amorphous, rugged state into another. From the practical point of view, such tolerance of mechanical pressure compensates for the lack of a refined pore structure and renders amorphous mesoporous silica a more appealing candidate for disk-shaped reactors and filters than any other silica species studied here.

Conclusions

In this contribution we have proved that generalizations about surface fractality should be made only with extreme care. By synthesizing three morphologically different samples and applying the standard fractal dimension calculations on them, we realized that even the same elemental composition (calcined silica) and same synthesis method (sol-gel route with organic additives) can lead to materials of totally different fractal behavior. Even the fractality of the same sample could be modified by applying mechanical pressure and thus ruining its morphology. On this basis we suggest that studies concerning surface scale invariance should include some morphological details as well, so that artifacts caused by the differing shapes of the investigated materials can be avoided.

Acknowledgment. We thank Dr. Y. Kiyozumi of NIMC, Tsukuba, Japan for some valuable SEM measurements. Financial support of the MKM FKFP grant No. 0486/1999 and the DAAD/MÖB project No. 30/1999 is gratefully acknowledged.

CM001168M